Molecular Orientation of Single and Two-Armed Monodendron Semifluorinated Chains on "Soft" and "Hard" Surfaces Studied Using NEXAFS

Jan Genzer,*,‡ Easan Sivaniah,‡ Edward J. Kramer,‡,§ Jianguo Wang,∥,⊥ Maoliang Xiang,∥ Kookheon Char,∥,# Christopher K. Ober,∥ Robert A. Bubeck,▽ Daniel A. Fischer,○,& Michael Graupe,^ Ramon Colorado, Jr.,^ Olga E. Shmakova,^ and T. Randall Lee^

Department of Chemical Engineering, North Carolina State University, Raleigh, North Carolina 27695-7905; Materials Department, University of California at Santa Barbara, Santa Barbara, California 93106-5050; Department of Materials Science & Engineering, Cornell University, Ithaca, New York 14853-1501; Michigan Molecular Institute, Midland, Michigan 48640; National Synchrotron Light Source, Brookhaven National Laboratory, Upton, New York 11973; Material Science & Engineering Laboratory, National Institute of Standards and Technology, Gaithersburg, Maryland 20899; and Department of Chemistry, University of Houston, Houston, Texas 77204-5641

Received October 13, 1999; Revised Manuscript Received May 4, 2000

ABSTRACT: Near-edge absorption fine structure (NEXAFS) measurements are used to probe the molecular orientation of semifluorinated (SF) mesogens, $-(CH_2)_x(CF_2)_yF$, which are attached to (i) the isoprene backbone of polyisoprene or a styrene-isoprene diblock copolymer ("soft" substrate), and (ii) a Au-covered solid substrate via a thiol link ("hard" substrate). The SF groups on both surfaces are oriented and on average are tilted from the sample normal. The tilt angle, $\langle\tau_{F-helix}\rangle$, of the fluorinated part of the SF group on each substrate is determined exclusively by the combination of x and y, increasing with increasing x and with decreasing y. Moreover, $\langle\tau_{F-helix}\rangle$ is found to be independent of the surface topology (flat surfaces vs surfaces covered with holes or islands of the copolymer), casting solvent, and the architecture of the SF group (single vs 2-armed monodendron). Comparing the orientation of the SF groups on both substrates reveals that $\langle\tau_{F-helix}\rangle$ is approximately 14° higher on the "soft" substrate.

1. Introduction

The current approach to the design of low surface energy materials is typically based on either attaching low surface energy groups onto hydrocarbon backbones[1−3] or blending polymers containing low surface energy moieties.[4−6] In principle, a homogeneously organized two-dimensional arrangement of trifluoromethyl ($-CF_3$) groups would be an ideal surface with very low surface energy. An example of polymeric materials that can form such surfaces are polymers with semifluorinated (SF) side groups $[-CO-(CH_2)_{x-1}-(CF_2)_yF]$.[7] These SF side groups exhibit liquid crystalline (LC) behavior as determined from independent differential scanning calorimetry and small-angle X-ray scattering (SAXS) experiments. In particular, X-ray diffraction measurements on these polymers show that the side groups are located in a highly ordered, LC smectic B (S_B) phase in the bulk. The immiscibility of the fluorinated groups with the hydrocarbon backbone (and the other block) and the LC nature of the side groups lead to the formation of structures whose surfaces are composed of highly ordered arrays of $-CF_3$ groups at the polymer/air interface. Previous experiments indicated clearly that these ordered assemblies show improvement in surface organization and enhancement in surface stability.[7−9] Films made of this SF side group block copolymer (e.g., $x = 4$, $y = 8$) had an extremely low critical surface tension (≈8 mJ/m^2) and were highly resistant to surface reconstruction in water (as measured by the receding water contact angle after prolonged water exposure).[7] In addition, near-edge X-ray absorption fine structure (NEXAFS) experiments showed that the SF side groups on the surfaces of the block copolymer thin films were highly organized and possessed an average angle of about 30° to the surface normal.[8]

Prior NEXAFS studies of fluorinated polyethers have shown the effect of the surface to direct orientation.[9a] The surface region induces the low surface energy fluorinated segments to orient toward air and avoid the alkyl underlayer, an effect similar to that observed in the materials described here. Similar effects of surface orientation have been observed in the case of fluorinated films grown using CVD processes,[9b] but these surfaces are subject to surface reconstruction. The SF side group block copolymers described in this paper have stable surface properties, but in contrast to the fluoroether surfaces, the polymer backbone to which the SF side groups are chemically attached has to have a high density of attachment sites (pendent vinyl groups sit

* Corresponding author. Present address: Department of Chemical Engineering, North Carolina State University, Raleigh, NC 27695-7905.
‡ University of California at Santa Barbara.
§ Also at: Department of Chemical Engineering, University of California at Santa Barbara, Santa Barbara, CA 93106-5080.
∥ Cornell University.
⊥ Present address: Polymer Core Technology, Corning Incorporated, Corning, NY 14831.
Permanent address: School of Chemical Engineering, Seoul National University, Seoul 151-744, Korea.
▽ Michigan Molecular Institute.
○ Brookhaven National Laboratory.
& National Institute of Standards and Technology.
^ University of Houston.

10.1021/ma991710w CCC: $19.00
Published on Web 07/13/2000

on every mer unit in the materials discussed above). It is of considerable interest to develop SF-group containing units with more than one SF-group per attachment site. Such groups could, in principle, also be attached to other surfaces including materials such as elastomer networks, in which there is lower density of attachment sites. This strategy could still achieve full surface coverage by the SF-units. Ober and co-workers have recently developed a versatile synthesis method to do this.[10] The SF-groups are incorporated as the outer units of a first generation, 2- or 3-branched monodendron.

The major thrusts of this work are 4-fold. First, we explore the effect of the chemical attachment of the SF groups to the polyisoprene (PI) backbone and compare the role of the single vs monodendron SF molecular structure. Second, we examine the effect of attachment density of the SF monodendron groups to the PI backbone on their surface orientation in thin SF films. Third, we investigate the effect of the casting solvent on the surface orientation of the SF groups. Finally, we compare the orientation of the SF groups attached to polymeric backbones ("soft substrates") with that of similar chemical moieties covalently bound to a solid substrate ("hard substrates"). To accomplish these tasks, we have applied scanning force microscopy to study the surface morphology of the SF polymer films and NEXAFS to investigate both the surface and interior orientation of the SF groups in such films.

2. Experiment

2.1. Materials and Sample Preparation. Diblock copolymers consisting of polystyrene (PS) and polyisoprene (PI) (60% of 1,2 and 40% of 3,4 PI units) blocks were synthesized using anionic polymerization and were used as the backbone to which the 2-armed monodendron SF side groups [HOCOC-$(CH_3)(CH_2OCO(CH_2)_{x-1}(CF_2)_yF)_2$] were attached by means of synthetic methods reported previously.[7] Two different SF monodendron copolymers (SFMDs) were prepared that differed in the degree of attachment of the 2-armed SF monodendron side groups, 66% and 40%, as determined from NMR spectroscopy.[11] We refer to them henceforth as M1-FyH*x* and M2-FyH*x*, respectively. The bulk morphology of the SF polymers consists of either spheres on the bcc lattice, hexagonally organized cylinders, or stacks of alternating lamellae depending on the volume fraction of the PS and the SF-PI blocks in the copolymer. These results were established by independent SAXS and transmission electron microscopy experiments.[7] Thin (≈50−80 nm) films of SFMDs were prepared by spin-coating solutions of the block copolymers onto silicon wafers. To uncover the role of the casting solvent on the orientation of the SF groups on the surfaces of the thin films, two different solvents were used, namely (i) α,α,α-trifluorotoluene (TFT), a good solvent for the SF−isoprene block; and (ii) a 50/50 (w/w) mixture of TFT and toluene (toluene is a good solvent for the PS block). The samples were subsequently annealed under vacuum at 150 °C for 4 h to perfect the surface and interior morphology.

Self-assembled monolayers consisting of semifluorinated alkanethiols, $HS-(CH_2)_{16-x}(CF_2)_xF$ with *x* ranging from 1 to 10, on gold-covered silicon wafers, SF-SAM (Au), were prepared. Many of the details of the SF synthesis have been reported;[12] complete analytical data for all new SF adsorbates will be reported separately.[13] The SF-SAM (Au) specimens were prepared by adsorption for 24 h from 1 mM solutions of the thiols in isooctane on gold-coated substrates that were prepared by evaporating gold (≈200 nm) onto silicon wafers precoated with chromium (≈10 nm). The chain orientation determined in these SF-SAM (Au) samples was used as a benchmark for interpreting our NEXAFS measurements on single chain and 2-armed monodendron SF side groups attached to polymeric backbones.

2.2. NEXAFS Experiments. NEXAFS was used to determine the surface and bulk orientation of the semifluorinated chains. We note that the tilt angle determined from NEXAFS represents an *average* value. There is no straightforward way to discriminate between the case of all chains homogeneously tilted by the same angle and the case of a disordered system with a broad distribution of tilt angles. We thus express our results on the orientation of the SF moieties in terms of the average tilt angle of the fluorocarbon part of the single SF groups, $\langle\tau_{F-helix}\rangle$. Moreover, due to the nature of the polarization dependencies of the NEXAFS signal intensities one cannot distinguish between a completely disoriented sample and a sample whose chains are all tilted by 54.7°, the so-called, "magic angle".[14]

The NEXAFS experiments were carried out on the U7A NIST/Dow materials characterization end-station at the National Synchrotron Light Source at Brookhaven National Laboratory. The principles of NEXAFS and description of the BNL beamline have been outlined elsewhere.[8,9b] The NIST/Dow materials characterization end-station is equipped with a heating/cooling stage positioned on a goniometer, which controls the orientation of the sample with respect to the polarization vector of the X-rays. A differentially pumped ultrahigh vacuum compatible proportional counter is used for collecting the fluorescence yield (FY) signal. In addition, the partial-electron-yield (PEY) signal is collected using a channeltron electron multiplier with an adjustable entrance grid bias (EGB). A crude depth profiling within the top 5 nm is made possible by increasing the negative EGB on the channeltron detector at the highest bias, thus selecting only the Auger electrons which have suffered negligible energy loss. The monochromator energy resolution and photon energy were calibrated by comparing the transmission spectrum from gas-phase carbon monoxide with electron energy-loss reference data. To eliminate the effect of incident beam intensity fluctuations and monochromator absorption features, the FY and PEY signals were normalized by the incident beam intensity obtained from the photo yield of a clean gold grid.

An important issue concerning the study of organic materials is the possibility of the sample damage during the characterization with UV light, X-ray and electron radiation.[15] Semifluorinated materials are particularly sensitive to these effects. Hence, a fresh area of the sample was exposed to the X-ray beam spot for each measurement to minimize possible beam damage effects. Moreover, NEXAFS spectra showed no damage effects for at least three consecutive runs taken from the same spot on the sample.

2.3. Contact Angle Measurements. Contact angle experiments were performed using a NRL contact angle goniometer 100−00 (Ramé-Hart Inc.).[16] Films were prepared from 2% α,α,α-trifluorotoluene solutions of the block copolymer using the method described earlier. After annealing in a vacuum at 150 °C for 4 h, the samples were cooled to room temperature at which the contact angles were measured. The contact angles reported later in the paper represent averages over four measurements. The advancing contact angles were read by injecting 4 μL liquid drops; the receding contact angles were determined by removing 3 μL of liquid from the droplet. Linear *n*-alkanes and low molecular weight methyl terminated poly(dimethylsiloxanes) were used as standards to construct Zisman plots.[17]

2.4. Transmission Electron Microscopy and Scanning Force Microscopy. The morphology of the block copolymer was investigated by transmission electron microscopy (TEM). Samples were stained using RuO_4 that reacts preferentially with the PS block. Thin films were microtomed from these samples and examined using a JEOL 1200 EX transmission electron microscope operating at 120 kV.[16] Scanning force microscopy (SFM) on the surfaces of these films was carried out using a Digital Instruments Nanoscope III in the tapping mode.[16]

3. Results and Discussion

Recently, we presented the results of a study of the morphological arrangement of PS-*b*-PI copolymers modi-

fied with single SF groups [$-OCO(CH_2)_{x-1}(CF_2)F$] attached to the PI block of the copolymer.[8] We showed that in contrast to the interior, where the SF-LC mesogens are aligned parallel to the polystyrene/SF-PI interface of the block copolymers, the surfaces of thin SF polymer films are covered with a uniform layer, consisting of the SF-LC groups that are only slightly tilted away from the sample normal. NEXAFS measurements revealed that the average tilt angle of the fluorocarbon part of the single SF groups, $\langle\tau_{F-helix}\rangle$, ranged from 29 to 46°, depending on x and y. Specifically, our NEXAFS results indicated that $\langle\tau_{F-helix}\rangle$ increased with increasing x and/or decreasing y. In this work, systematic NEXAFS measurements were carried out on related block copolymers with semifluorinated 2-armed monodendron groups (samples M1-FyHx and M2-FyHx) to establish $\langle\tau_{F-helix}\rangle$ for this new architecture and to investigate the role of attachment density of the 2-armed monodendron SF groups on the PI backbone.

By simultaneously detecting both the PEY and FY signals, whose probing depths are ≈2 and ≈100 nm, respectively, we have demonstrated that the orientation of the SF groups on the surface and in the interior can be resolved.[8] In particular, we showed that both PEY and FY signals reveal the presence of peaks corresponding to the 1s → σ^* transitions associated with the C−H, C−F, and C−C bonds. In addition, one more strong peak was present in the FY spectrum but was absent in the PEY data. This peak, detected at E = 284.5 eV, was associated with the 1s → π^* transition of the PS phenyl ring. Thus, by comparing the information obtained from the PEY and FY spectra, we concluded that the surfaces of the SF thin films with the single SF side groups attached to the copolymer backbone, were composed of only the SF-PI moieties. Because no signal that would indicate the presence of PS on the surfaces of the SF thin films was detected, our results showed clearly that the SF groups at the surface were densely packed. While the attachment of the 2-armed SF monodendron groups to the copolymer was carried out using the same chemistry as that of single SF side groups, the degree of substitution on the polymer backbone was chosen to be less than 100%.

We were thus interested in how this difference influences the density of the SF groups on the surfaces of thin SF polymer films. Figure 2 shows the PEY (upper part) and FY (lower part) NEXAFS signals from the M1-F8H10 (66% attachment) sample positioned perpendicular to the X-ray beam (θ = 90°). As expected, both PEY and FY NEXAFS spectra contain the signals that correspond to the 1s → σ^* transitions associated with the C−H (E = 287.9 eV), C−F (E = 292.0 eV), and C−C (E = 294.8 eV) bonds. However, a strong signal from the 1s → π^* transition of the PS phenyl ring at E = 284.5 eV is detected only in the FY NEXAFS scan. This result thus demonstrates that few PS segments are present at the sample surface. Similar conclusions can be reached when inspecting the PEY and FY NEXAFS scans from M2-F8H10 (40% attachment), shown in Figure 3, taken under the same experimental conditions as those of M1-F8H10. Again the extremely weak 1s → π^* transition signal from the PS phenyl ring at E = 284.5 eV in the PEY NEXAFS spectrum and its strong presence in the FY NEXAFS spectrum of M2-F8H10 suggests that the vast majority of PS segments are "buried" at least 2 nm inside the sample. These results thus suggest that the surfaces of the SFMD films are composed of densely packed SF chains despite the lower extent of substitution of the 2-armed SF monodendron groups on the PI backbone as compared to those of the single-chain SF groups.

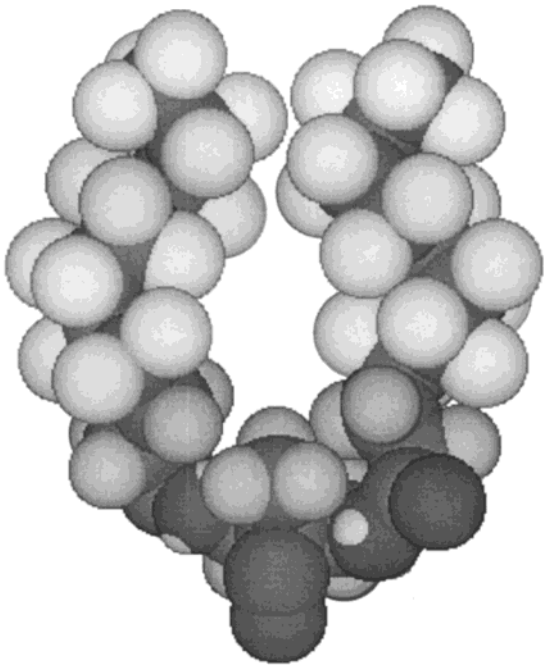

Figure 1. Chemical structure of two-armed semifluorinated monodendron group with the structure $-OCOC(CH_3)(CH_2-OCO(CH_2)_2(CF2)_6F)_2$.

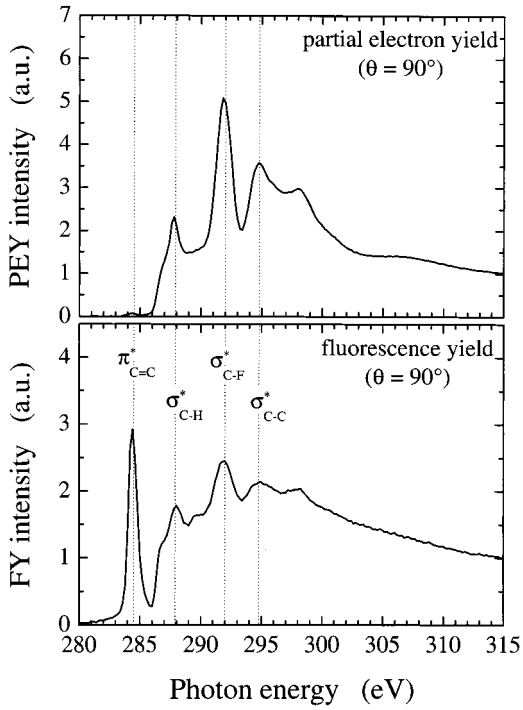

Figure 2. PEY (upper part) and FY (lower part) NEXAFS spectra (solid lines) from M1-F8H10 sample at EGB = −150 V and θ = 90°. The dotted lines in the figure denote the 1s → σ^* transitions for the C−H (E = 287.9 eV), C−F (E = 292.0 eV), and C−C (E = 294.8 eV) bonds (present in both the PEY and FY NEXAFS spectra) and the 1s → π^* transition of the PS phenyl ring (E = 284.5 eV) present only in the FY NEXAFS spectrum.

Contact angle measurements represent perhaps the easiest, quickest, and most reliable method of determining surface properties, such as wettability, of materials.

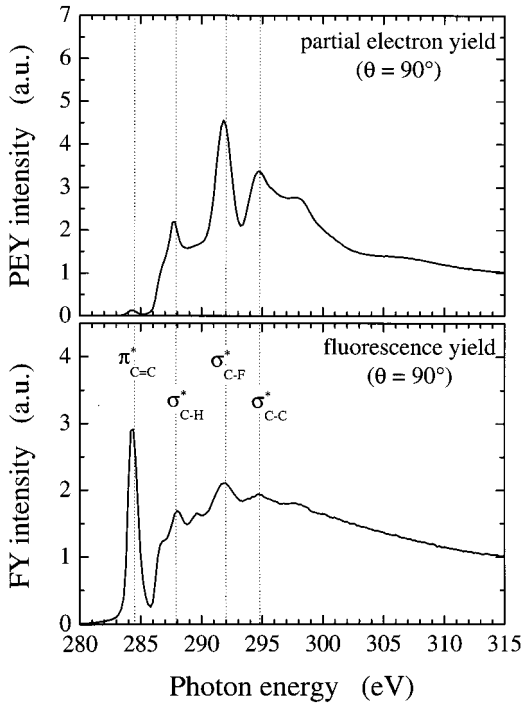

Figure 3. PEY (upper part) and FY (lower part) NEXAFS spectra (solid lines) from M2-F8H10 sample at EGB = −150 V and $\theta = 90°$. The dotted lines in the figure denote the 1s → σ^* transitions for the C−H ($E = 287.9$ eV), C−F ($E = 292.0$ eV), and C−C ($E = 294.8$ eV) bonds (present in both the PEY and FY NEXAFS spectra) and the 1s → π^* transition of the PS phenyl ring ($E = 284.5$ eV) present only in the FY NEXAFS spectrum.

Table 1. Room-Temperature Advancing and Receding H_2O Contact Angles on H-F8H10, BC-F8H10, M1-F8H10, M2-F8H10, and BC-F8H10 Samples

sample	advancing θ_{H_2O} (deg)	receding θ_{H_2O} (deg)
H-F8H10	122 ± 1	112 ± 1
BC-F8H10	122 ± 1	110 ± 1
M1-F8H10	120 ± 1	110 ± 1
M2-F8H10	120 ± 1	108 ± 1
BC-F8H4	120 ± 1	109 ± 1

Contact angle experiments, similar to those reported previously,[7] were carried out on Z−F8H10 samples, where Z was either "H" (a PI homopolymer—H-F8H10), or "BC" (a PS-*b*-PI block copolymer—BC-F8H10), or "M1" (M1-F8H10), or "M2" (M2-F8H10). Table 1 lists water contact angle data collected from these samples with the result from the BC-F8H4 sample added for comparison.[7] The data in Table 1 demonstrate that within experimental error, the wetting properties of all samples are essentially the same. The small (≈10°) water contact angle hysteresis, the difference between the advancing and receding water contact angles, is the same for all samples. This small value indicates excellent surface packing of the LC−SF chains. Previously, we used Zisman plots to obtain estimates of γ_{crit}, the critical surface energies of the SF materials. These measurements revealed very low surface energies (≈8 mJ/m^2) consistent with close packing of $-CF_3$ groups at the surfaces of the SF thin films.[7] Similar experiments were carried out on the M1-F8H4 and M2-F8H4 samples. Figure 4 shows a Zisman plot for M1-F8H4 that was generated from the contact angles measured using a series of *n*-alkanes and methyl-terminated poly(dimethylsiloxanes).[18] The value of γ_{crit} extracted from the data (≈8.2 mJ/m^2) is exactly the same as that

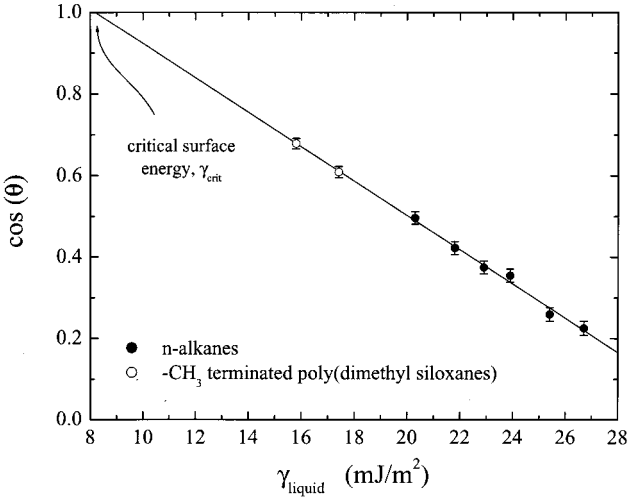

Figure 4. Zisman plot for M1-F8H10 constructed from contact angle measurements using a homologous series of *n*-alkanes (closed circles) and methyl-terminated poly(dimethylsiloxanes) (open circles).[18]

reported previously for BC-F8H10.[7] Thus, the excellent agreement between the contact angle data (both the water contact angles and γ_{crit}) for the single and the monodendron SF groups implies that changing the means of attachment of a SF side group to the polymer backbone (while keeping *x* and *y* the same) does not influence the surface properties of SF thin films. While providing a useful first insight into surface properties of the SF materials, contact angle measurements cannot furnish information about the molecular orientation of the SF chains on the SF-polymer surfaces. On the other hand, as we demonstrated earlier,[8] one can resolve the molecular orientation of the SF groups on the SF film surfaces using NEXAFS.

NEXAFS experiments were carried out at eight different orientations of the sample with respect to the incident X-ray beam, θ, ($\theta = 20$, 30, 40, 55, 60, 70, 80, and 90°).[8] To obtain the dependence of the intensities of the 1s → σ^* transitions corresponding to the C−H, C−F, and C−C bonds, the resulting PEY NEXAFS spectra were then fitted to a series of Gaussian curves and a step corresponding to the excitation edge of carbon following the method proposed by Outka and co-workers.[19] Figure 5 shows the normalized PEY 1s → σ^* C−F bond NEXAFS intensities vs θ from the C 1s edge of the SF-LC 2-armed monodendron groups in M1-F8H10 (closed squares) and M2-F8H10 (open squares). To compare the orientation of the 2-armed SF monodendron side groups with those of single SF side groups, the results for the orientation of the latter moieties (with the same chemical composition) attached to H-F8H10 (closed circles) and BC-F8H10 (open circles) are also included in Figure 5. The latter two data sets have already been presented and discussed in our previous publication.[8] Also included in Figure 5 are the data for a semifluorinated self-assembled monolayer [$-O_{1.5}Si-(CH_2)_2-(CF_2)_8F$] on SiO_x, SF-SAM (SiO_x) (crosses).[8] Figure 5 reveals two important and interesting pieces of information. First, the fact that the data from the SF groups attached to the PI backbone collapse onto a single master curve indicates that the average tilt angles of the fluorocarbon part of the molecule are the same for both the single and 2-armed monodendron SF groups. Second, the results in Figure 5 illustrate that $\langle\tau_{F-helix}\rangle$ for the SF-SAM (SiO_x) sample is smaller than

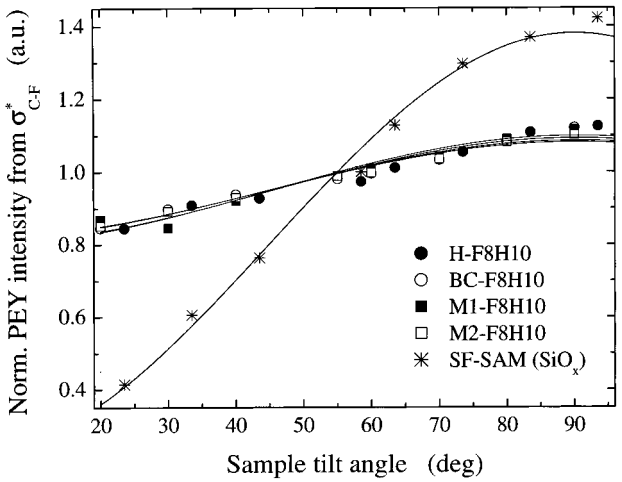

Figure 5. Normalized PEY NEXAFS intensities vs sample tilt angle from σ^* C−F bond in C 1s edge of SF-SAM (SiO_x) (stars), H-F8H10 (closed circles), BC-F8H10 (open circles), M1-F8H10 (closed squares), and M2-F8H10 (open squares). The solid lines were obtained by fitting the experimental data using the "modified building block" model method described in ref 20.

Table 2. Average Tilt Angles of the Fluorocarbon Helix for H-F8H4, BC-F8H10, M1-F8H10, and M2-F8H10 Samples

sample	preparation conditions[a]	$\langle\tau_{F-helix}\rangle$ (deg)
H-F8H10	TFT cast	43.7 ± 3.8
BC-F8H10	TFT cast	43.0 ± 3.1
M1-F8H10	TFT cast	41.2 ± 3.6
M1-F8H10	TFT/Tol (50/50 w/w) cast	42.5 ± 3.2
M2-F8H10	TFT cast (8/1998)	41.9 ± 3.9
M2-F8H10	TFT/Tol (50/50 w/w) cast	44.8 ± 3.3

[a] Samples were cast from either from either α,α,α-trifluorotoluene (TFT) or a 50/50 (w/w) α,α,α-trifluorotoluene/toluene (TFT/Tol) mixture.

that for the polymer specimens, in agreement with the previously reported behavior.[8] The steeper the slope of the intensity vs sample tilt angle, the smaller is the average tilt $\langle\tau_{F-helix}\rangle$ of the $-(CF_2)_y-$ helix from the substrate normal.[8] The lines in Figure 5 represent the fits to the experimental data using the model described in ref 20. The results in Figure 5 thus clearly reveal one important conclusion, namely that the dominant driving force that dictates the orientation of the SF groups on the surfaces of thin polymer films is the molecular structure (given by the combination of *x* and *y*) of the LC chains and not the form of their attachment to the polymeric backbone. The numerical values of $\langle\tau_{F-helix}\rangle$ obtained from these fits will be reported later in the paper (cf. Table 2).

As pointed out earlier, due to very different solubilities of fluorocarbons and hydrocarbons, it is usually difficult to find a common solvent for both fluorocarbon and hydrocarbon species. Using a solvent that dissolves one component well and does not dissolve the other, however, may lead to solvent-specific polymer morphologies. Evidence of the solvent effect on the bulk morphologies of the SF polymers comes from transmission electron microscopy (TEM) and scanning force microscopy (SFM) experiments. Figure 6 shows TEM images taken from BC-F8H10 samples cast from (a) α,α,α-trifluorotoluene (TFT), and (b) tetrahydrofuran (THF). Both samples were annealed for 21 days at 140 °C, microtomed and stained with RuO_4 that selectively

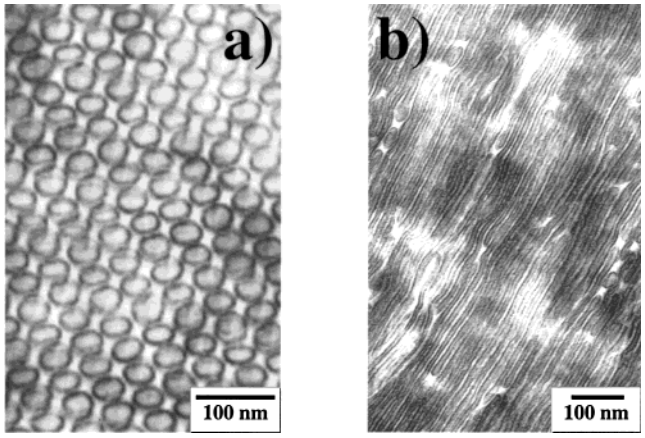

Figure 6. Transmission electron microscopy images of BC-F8H10 cast from (a) α,α,α-trifluorotoluene, and (b) tetrahydrofuran.

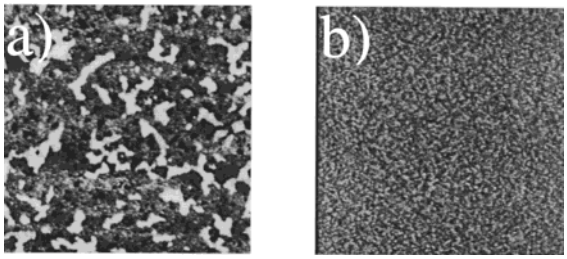

Figure 7. Scanning force microscopy images of the surfaces of BC-F8H4 cast from (a) α,α,α-trifluorotoluene, and (b) a 50/50 (w/w) α,α,α-trifluorotoluene/toluene mixture. The length of the edge of each picture corresponds to 30 μm.

stains only the PS block. Figure 6 shows clearly that the morphology of BC-F8H10 depends on casting solvent. Specifically, Figure 6a and independent SAXS experiments indicate that samples cast from TFT exhibit a hexagonal morphology with the cylinders being composed of the PS block and the SF-PI phase forming the matrix. Recalling that TFT is a better solvent for SF-PI than for PS, this arrangement indicates that the PS block collapses inside the solvated SF-PI block. On the other hand, when THF, which is a good solvent for the PS block, is used as the casting solvent, alternating PS and SF-PI lamellae (cf. Figure 6b) is the resultant sample morphology. This example illustrates that because the sample bulk morphology changes with casting solvent, one has to be concerned about the influence of the casting solvent on the morphology of surfaces of thin SF films. Figure 7 shows SFM images taken from BC-F8H4 samples prepared by spin-coating polymer solution (a) in TFT, and (b) a 50/50 (w/w) mixture of TFT and toluene (Tol), a solvent for the styrene block. As apparent from the images, the topography of the sample surface also depends on the casting solvent. The root-mean-squared roughnesses determined from the SFM images are approximately 23.1 and 6.7 nm for the TFT and TFT/Tol cast samples, respectively. By analogy to the bulk morphology discussed above, the different surface morphology observed in Figures 7a and 7b can also be attributed to the differences in the solubilities of the two blocks in TFT and the TFT/Tol mixture. Since TFT is a better solvent for the SF-containing species, the SF-PI block will be more swollen as compared to PS and the resultant morphology will reflect the larger volume of the SF-PI block. On the other hand, when using TFT/Tol mixtures, both blocks should be swollen

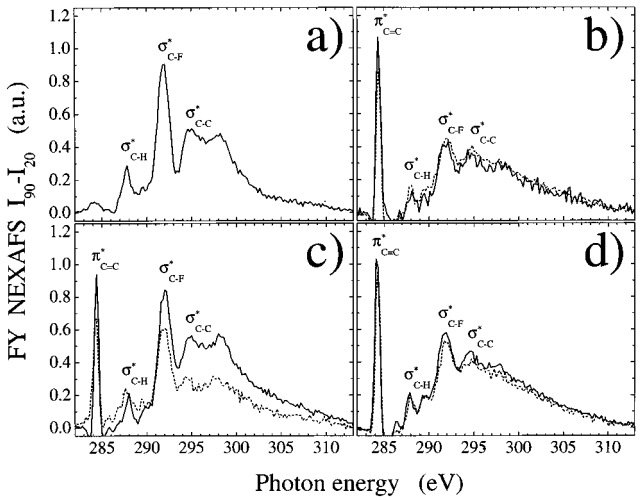

Figure 8. Difference FY NEXAFS intensities (obtained by subtracting the FY NEXAFS spectra taken at $\theta = 90°$ and $\theta = 20°$) for (a) H-F8H10, (b) BC-F8H10, (c) M1-F8H10, and (d) M2-F8H10. The solid lines represent the data taken from samples cast from α,α,α-trifluorotoluene and the dotted lines depict the data obtained from the samples prepared from 50/50 (w/w) α,α,α-trifluorotoluene/toluene mixtures.

which in turn leads to fine grain size, as demonstrated by the image in Figure 7b. Because of the solvent-selective bulk and surface morphologies, we were interested in finding out to what extent the solvent quality affects the organization of the SF groups on the surfaces of thin films.

Earlier in the paper, we pointed out that one of the strengths of NEXAFS is its ability to simultaneously probe both the interior and surface structure of material. In the present study we use a FY NEXAFS signal to probe the interior of thin SF films and the PEY NEXAFS signal to examine the orientation of the SF groups at the film surfaces. Figure 8 shows the FY difference NEXAFS spectra from (a) H-F8H10, (b) BC-F8H10, (c) M1-F8H10, and (d) M2-F8H10 cast from either TFT (solid line) or a 50/50 (w/w) TFT/Tol mixture (dotted line). The spectra in Figure 8 were obtained by subtracting the normalized FY NEXAFS spectra recorded at $\theta = 90°$ and $\theta = 20°$. The assignment of the residual peaks present in the difference FY NEXAFS spectra in Figure 8 is the same as that in Figures 2 and 3, namely, $E(\pi^*_{C=C}) = 284.5$ eV, $E(\sigma^*_{C-H}) = 287.9$ eV, $E(\sigma^*_{C-F}) = 292.0$ eV, and $E(\sigma^*_{C-C}) = 294.9$ eV. Let us first concentrate on the TFT-cast samples (solid lines in Figure 8). The data in Figure 8 reveals that there are two different patterns in the FY NEXAFS peaks, suggesting the existence of two different types of bulk morphologies. Namely, the H-F8H10 and M1-F8H10 samples appear to have similar bulk structure. Also, the similarity between the shapes of the BC-H8H10 and the M2-F8H10 FY spectra hints that these two samples have similar structures (but different from those of H-F8H10 and M1-F8H10). This observation is interesting considering that the orientation of the SF mesogens at the surfaces of these samples is essentially identical, as revealed by their identical PEY NEXAFS signals (cf. Figure 5). Now turning to the data from TFT/Tol-cast samples (dotted lines in Figure 8), another intriguing observation can be made. Namely, while the internal morphology of the M1-F8H10 sample seems to be altered when cast from TFT/Tol mixtures as compared to the TFT-cast sample, using different solvents does not seem to make too much of a difference in the case of the M2-F8H10 sample. Clearly, the interplay between the different degrees of attachment of the SF monodendron groups and the solvent quality has some effect on the orientation of the SF groups in the polymer film. The FY NEXAFS data thus reinforces the information previously obtained by TEM and SFM.

Table 3. Average Tilt Angles of the Fluorocarbon Helix for H-F8H4 and BC-H8H4 Samples

sample	preparation conditions[a]	$\langle\tau_{F-helix}\rangle$ (deg)
H-F8H4	TFT cast	29.1 ± 2.9
BC-F8H4	TFT cast[b]	33.0 ± 3.0
BC-F8H4	TFT cast[b]	31.1 ± 3.1
BC-F8H4	TFT/Tol (50/50 w/w) cast	34.8 ± 3.9

[a] Samples were cast from either from either α,α,α-trifluorotoluene (TFT) or a 50/50 (w/w) α,α,α-trifluorotoluene/toluene (TFT/Tol) mixture. [b] Samples measured 1 year apart.

On the basis of the SEM, SFM, and FY NEXAFS results, one would expect the orientation of the SF groups on the surfaces of the SF polymers to also depend on casting solvent. Table 2 summarizes the results for $\langle\tau_{F-helix}\rangle$ obtained from the PEY NEXAFS measurements on H-F8H4, BC-F8H10, M1-F8H10, and M2-F8H10 samples cast from either TFT or a 50/50 (w/w) TFT/Tol mixture. Surprisingly, $\langle\tau_{F-helix}\rangle$ appears to be almost identical for all specimens investigated regardless of the nature of the SF groups (single vs 2-armed monodendron), polymer backbone (homopolymer vs copolymer) and casting solvent. Specifically, $\langle\tau_{F-helix}\rangle$ ranges from 41.2 ± 3.6° for M1-F8H10 TFT-cast sample to 44.8° ± 3.3° for M2-F8H10 50/50 (w/w) TFT/Tol-cast specimen. To verify that this behavior is not a specific feature of the F8H10 moiety, in Table 3 we present $\langle\tau_{F-helix}\rangle$ for H-F8H4 and BC-F8H4 cast from different solvents. Also here $\langle\tau_{F-helix}\rangle$ is almost the same for all samples, ranging from 29.1 ± 2.9° for the H-F8H4 TFT-cast sample to 34.8 ± 3.9° for the BC-F8H4 specimen spin-coated from the 50/50 (w/w) TFT/Tol mixture. Moreover, the data in Table 3 illustrate both the high reproducibility of the NEXAFS measurements and the stability of the SF surfaces; $\langle\tau_{F-helix}\rangle$ values determined from the PEY NEXAFS signal on TFT-cast F8H4 samples measured one year apart is almost *indistinguishable*.

Many experiments on diblock copolymer thin films carried out over the past eight years revealed clearly that when confined in thin film geometry, the lamellar structure can be either homogeneous (parallel to surface) or homeotropic (perpendicular to surface).[21] While the homeotropic structure is expected to occur only in systems in which both components exhibit the same interaction energies at the interface with the outside medium, a homogeneous morphology will be present when either of the two blocks exhibits a preferential attraction to that interface. Moreover, while for the homeotropic case the surface always remains flat, the surface topography of homogeneous structures whose one block wets both interfaces will only remain flat when the total film thickness is nL_o (where n is an integer and L_o is the period of the lamellar structure). For any other thicknesses, the film surface will be covered with either holes or islands. Similarly, homogeneous block copolymer films whose two different blocks partition at the two interfaces will stay flat only if their thickness satisfies the commensurability condition given by $(n + {}^1/_2)L_o$, and will be covered by either islands or holes for other thicknesses. Figure 9 shows the sequence of four images taken using SFM from the

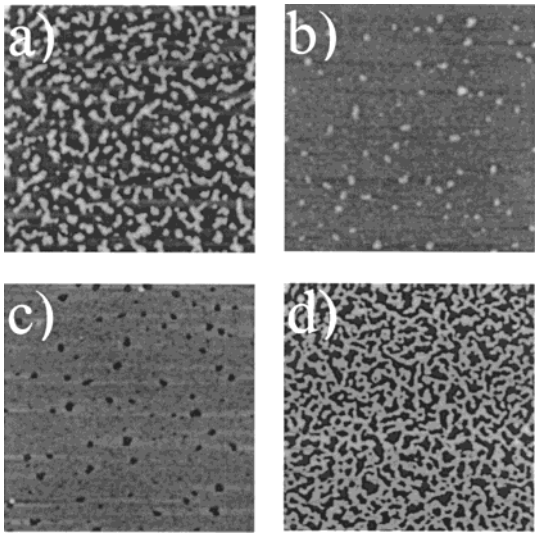

Figure 9. Scanning force microscopy images of the surfaces of the BC-F8H10 sample, which was prepared by spin-coating the 50/50 (w/w) α,α,α-trifluorotoluene/toluene mixture solutions of various concentrations onto silicon wafers. The thicknesses of the samples as measured using ellipsometry were: (a) 102.7, (b) 84.5, (c) 72.5, and (d) 53.5 nm. The length of the edge of each picture corresponds to 35 μm.

surfaces of BC-F8H10 samples cast from a 50/50 (w/w) TFT/Tol mixture with film thicknesses of (a) 102.7, (b) 84.5, (c) 72.5, and (d) 53.5 nm as measured by ellipsometry. The existence of islands and holes on the surface indicates that the orientation of the SF-PI and PS blocks is homogeneous with the PS block present at the polymer/solid interface and the SF-PI block partitioning at the film surface. Image analysis reveals that $L_o \approx$ 53 nm. Ideally, one would carry out the NEXAFS experiments on samples with flat surfaces to avoid complications arising from the nondesirable scattering effects caused by the existence of islands or holes. Our NEXAFS experiments on samples whose surfaces were covered by either islands or holes resulted in the same value of $\langle \tau_{F-helix} \rangle$ as those of experiments on samples with flat SF surfaces. Thus, the different surface topology caused by thickness quantization does not seem to affect the molecular orientation of the SF groups on the surfaces of the SF block copolymer films.

To interpret the orientation of the SF groups attached to the polymeric backbones and specifically to address the role of the attachment points between the SF groups and the PI polymer, we performed a comprehensive NEXAFS study of the orientation of SF alkanethiols, in the form of self-assembled monolayers, attached to gold-covered solid substrates, SF-SAM (Au).[13,22] Thiols were synthesized with compositions of the general formula $HS(CH_2)_{16-y}(CF_2)_yF$ with y ranging from 1 to 10, and from these thiols, the SF-SAM surfaces were prepared on gold.[12,13] The chemical composition of the SF-SAM (Au) moieties was chosen so that it produced a chemical architecture similar to the SF groups attached to the PI backbone discussed in this paper. Figure 10 shows the PEY NEXAFS yields from SF-SAM (Au) measured at an entrance grid bias of −150 V for (a) $\theta = 90°$ and (b) $\theta = 20°$. To simplify the nomenclature, we refer to the samples as FyH16−y. The data in Figure 10a show that, in samples positioned perpendicular to the X-ray beam ($\theta = 90°$), the intensity of the σ^*_{C-F} signal gradually increases with increasing number of $-CF_2-$ groups in the monolayer and levels off

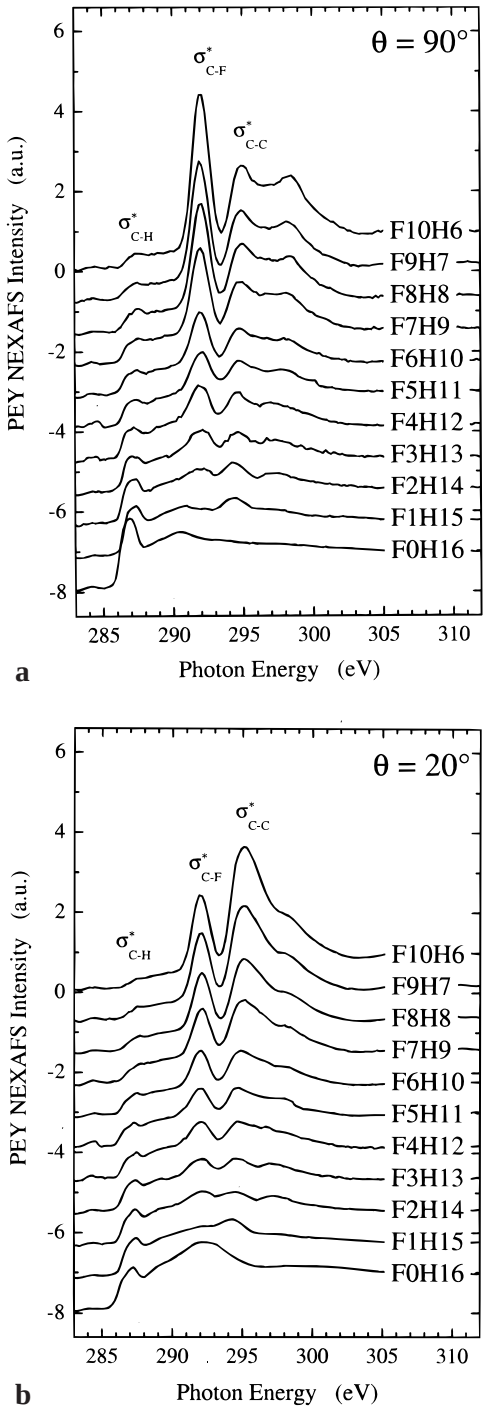

Figure 10. PEY NEXAFS spectra of SF-SAM (Au) samples at EGB = −150 V and (a) $\theta = 90°$ and (b) $\theta = 20°$. In the nomenclature used, FyHx corresponds to a $HS(CH_2)_{16-y}(CF_2)_yF$ moiety.

for $y \geq 7$. This trend is in agreement with IR measurements presented elsewhere.[13] Moreover, Figure 10a reveals that for $y \geq 4$ the σ^*_{C-F} signal intensity is higher than that corresponding to σ^*_{C-C} at $\theta = 90°$. Figure 10b shows the PEY NEXAFS spectra from samples whose surfaces are oriented almost parallel with respect to the X-ray beam ($\theta = 20°$). For $\theta = 20°$, the intensity of the σ^*_{C-F} signal also gradually increases with increasing number of $-CF_2-$ groups in the monolayer and levels off for $y \geq 7$. In addition, for $y \geq 4$ the σ^*_{C-F} signal intensity is lower than that corresponding to σ^*_{C-C}. A comparison of the data at both sample tilt angles reveals

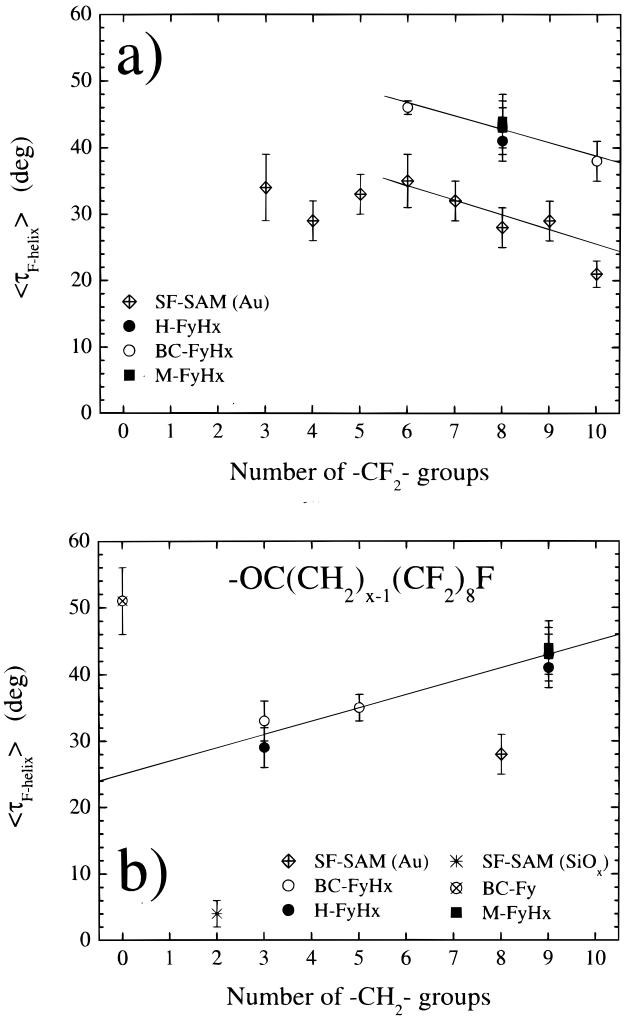

Figure 11. Average tilt angles of the fluorocarbon helix, $\langle\tau_{F-helix}\rangle$, for SF-SAM (Au) (crossed diamonds), SF-SAM (SiO_x) (crosses), BC−F*y*H*x* (open circles), BC−F*y* (crossed circles), H-F*y*H*x* (closed circles), and M-F*y*H*x* (closed squares) as a function of (a) the number of the $-CF_2-$ units and (b) the number of the $-CH_2-$ units (for $y = 8$) in the SF side group. The solid lines are guides to the eye.

that the SF-SAM (Au) monolayer is oriented for $y \geq 4$. The $\langle\tau_{F-helix}\rangle$ from the SF-SAM (Au) samples from the PEY NEXAFS measurements was evaluated using the procedure outlined above. A detailed analysis of the molecular orientation of the SF-SAM (Au) groups on Au-covered silicon substrates can be found in ref 13.

By determining $\langle\tau_{F-helix}\rangle$ for both the Z-F*y*H*x* samples (where Z is "BC", "H", or "M") and the SF-SAM (Au) specimens, the role of the substrate ("soft" vs "hard") on the orientation of the SF groups can be elucidated. The results summarizing the $\langle\tau_{F-helix}\rangle$ values of SF chains on "soft" (polymer) and "hard" (Au-covered wafer) substrates are presented in Figure 11. Figure 11 shows the $\langle\tau_{F-helix}\rangle$ values determined from PEY NEXAFS measurements on SF-SAM (Au) (crossed diamonds), SF-SAM (SiO_x) (cross), BC−F*y*H*x* (open circles), BC−F*y* (crossed circles), H-F*y*H*x* (closed circles), and M-F*y*H*x* (closed squares). In Figure 11a, we plot $\langle\tau_{F-helix}\rangle$ as a function of the number of the $-CF_2-$ units in the SF group. The data show that for the SF groups attached to both the "soft" and "hard" substrates $\langle\tau_{F-helix}\rangle$ decreases with increasing *y*. Moreover, for $y \geq 6$, $\langle\tau_{F-helix}\rangle$ on the "hard" surface is consistently about 14° lower that that for the SF groups attached to the "soft" substrates. The general trends are indicated by the solid lines that are only meant to guide the eye. To illustrate the effect of *x* on the surface orientation of the SF groups on both the "soft" and "hard" substrates, we present in Figure 11b $\langle\tau_{F-helix}\rangle$ for $y = 8$ as a function of the number of the $-CH_2-$ units in the SF group. The data in Figure 11b show that $\langle\tau_{F-helix}\rangle$ increases with increasing *x*. A close inspection of the results reveals that $\langle\tau_{F-helix}\rangle$ for the "soft" substrate sample follows a straight line and also reinforces the results discussed earlier in the paper, namely that $\langle\tau_{F-helix}\rangle$ does not depend on the chemical nature of the polymeric backbone (copolymer vs homopolymer) nor does it depend on the SF group architecture (single chain vs monodendron). As already discussed in the description of the results presented in Figure 11a, $\langle\tau_{F-helix}\rangle$ for the SF groups attached to the "soft" substrates is approximately 14° higher than that for "hard" substrates. There are two exceptions to the linear dependence of $\langle\tau_{F-helix}\rangle$ on the number of the $-CH_2-$ units in the SF group, however. First, as shown in Figure 11b, the value of $\langle\tau_{F-helix}\rangle$ for the BC−F8 sample (=51 ± 5°) is close to the NEXAFS "magic angle" (=54.7°) suggesting that the $-OCO(CF_2)_8F$ molecules on the surface of the BC−F8 sample are completely disordered.[8,22] Recalling that unlike the BC−F*y*H*x* specimens, the BC−F8 sample did not exhibit any bulk LC behavior,[7] the lack of orientation of the $-OCO-(CF_2)_8F$ side group is perhaps not so surprising. Second, the average tilt of the SF helix on the surface of SF-SAM (SiO_x) also deviates from the previously described trend. The fact that the SF part of the molecule in the SF-SAM (SiO_x) sample lies more nearly normal to the surface in contrast to the orientation of the SF-thiol molecules in principle could be attributed to two factors: (i) short hydrocarbon spacer and (ii) a different bonding environment of the SF molecule on the substrate. However, previous NEXAFS and grazing incidence infrared spectroscopy measurements on self-assembled monolayers of $F(CF_2)_8C(O)N(H)(CH_2)_2SH$ on Au showed that the $-CF_2-$ helix is also oriented normal to the substrate just as it is for our SF-SAM (SiO_x).[23] Thus, the helix tilt we observe for SF-SAM (Au) must be due to the extra $-CH_2-$ groups in these monolayers. This conclusion is in excellent agreement with recent polarized IR measurements on monolayer films of $F(CF_2)_8(CH_2)_{11}SH$ on Au.[24]

The results presented in this work clearly demonstrate that the orientation of the SF-LC groups on the surfaces of thin polymer films is controlled by the chemical architecture of the SF groups. Moreover, we found that the means of attachment of the SF groups to the polyisoprene block (single vs monodendron), the nature of the polymeric backbone (homopolymer vs copolymer), and the casting solvent play only minor roles in influencing the surface arrangement of the SF-LC moieties in the SF polymer films. These results reinforce the findings reported in our previous publication that the average tilt of the fluorocarbon part of the single SF groups attached to a polymeric backbone is determined by a combination of *x* and *y* and is thus dictated by the molecular structure of the SF group.[8,9]

Comparing the values of $\langle\tau_{F-helix}\rangle$ from the SF-groups attached to polymeric backbones and solid surfaces reveals that, in addition to the combination of *x* and *y*, the molecular orientation of the SF groups is also controlled by the nature of the attachment of these

groups to the substrate. Numerous prior studies on the orientation of self-assembled monolayers made of ω-functionalized alkanethiols [$HS-(CH_2)_x-\omega$] attached to different solid substrates revealed that the average tilt of chains with a fixed x and ω depends on the chemical nature of the substrate.[25−27] For example, the average tilt of $HS(CH_2)_xCH_3$ from the sample normal attached to polycrystalline gold is approximately 30−35°.[25,27] However, when deposited onto a silver-covered substrate the same chemical moiety was found to be oriented almost perpendicular to the sample surface.[26] This distinct behavior was attributed to the difference in the orientation of the Au−S and Ag−S bonds and the spacing of the Au and Ag atoms on the surface.[27] These experiments thus indicated that in addition to the chemical composition of the surface chemical modifier, the orientation within the self-assembled monolayer composed of such chain depends also on the nature of the chain attachment to the substrate.

4. Conclusion

In this paper, we presented and discussed the results of NEXAFS experiments that had the goal of elucidating the molecular orientation of semifluorinated (SF) mesogens, $-(CH_2)_x(CF_2)_yF$, attached to the isoprene backbone of either homopoly(isoprene) or a styrene-isoprene diblock copolymer ("soft" substrate), and a Au-covered solid substrate via a thiol link ("hard" substrate). Our results show conclusively that the SF groups on both surfaces are oriented and are tilted on average from the sample normal. The tilt angle, $\langle\tau_{F-helix}\rangle$, of the fluorinated part of the SF group is found to be independent of the surface topology (flat surfaces vs surfaces covered with either holes or islands of the copolymer), casting solvent, and the architecture of the SF group (single vs 2-armed monodendron). While for $y \geq 6$, the general trend in the behavior of $\langle\tau_{F-helix}\rangle$ on both surfaces is the same, $\langle\tau_{F-helix}\rangle$ on the "soft" surface is consistently about 14° higher. Overall, $\langle\tau_{F-helix}\rangle$ of the fluorinated part of the SF group on each substrate is determined exclusively by (i) the combination of x and y ($\langle\tau_{F-helix}\rangle$ increases with increasing x and with decreasing y) and (ii) the bonding environment of the SF group at the substrate.

Acknowledgment. This research was supported by the Office of Naval Research, Grant No. N00014-92-J-1246. Partial support from Division of Materials Research, NSF Polymer Program, Grants No. DMR92-23099 and DMR93-214573, is also appreciated. This work made use of MRL Central Facilities at UCSB supported by the National Science Foundation under award no. DMR96-32716. The work at NC State University was supported by the NCSU COE start-up funds and the NSF CAREER award, Grant No. DMR98-75256. The work at the University of Houston was supported by the National Science Foundation, Grant No. DMR97-00662. K.C. greatly acknowledges the financial support from the LG-Yonam Foundation for a sabbatical visit to Cornell University (1997−1998). NEXAFS experiments were carried out at the National Synchrotron Light Source, Brookhaven National Laboratory, which is supported by the U. S. Department of Energy, Division of Materials Sciences and Division of Chemical Sciences. The authors thank Prof. Manoj K. Chaudhury (Lehigh University) for providing the SF-SAM (SiO_x) sample, Mr. Xuefa Li (Cornell University) for his electron microscopy studies of the SF polymers, Dr. Benjamin M. DeKoven (Intevac), Dr. B. Glüsen, Dr. S. Yang (both Cornell University), and Dr. Sharadha Sambasivan (Brookhaven National Laboratory) for their assistance during the course of the experiments.

References and Notes

(1) Katano, Y.; Tomono, H.; Nakajima, T. *Macromolecules* **1994**, *27*, 2342. Hopken, J.; Möller, M. *Macromolecules* **1992**, *25*, 1461. Schneider, J.; Erdelen, C.; Ringsdorf, H.; Rabolt, J. T. *Macromolecules* **1989**, *22*, 3475. Rabolt, J. F.; Russell, T. P.; Tweig, R. J. *Macromolecules* **1984**, *17*, 2786.

(2) Schmidt, D. L.; Coburn, C. E,; DeKoven, B. M.; Potter, G. E.; Meyers, G.; F.; Fisher, D. A. *Nature* **1994**, *368*, 39.

(3) Pittman, A. G. In *Fluoropolymers*; Wall, L. A., Ed.; Wiley: New York, 1972; Vol. 25, p 419.

(4) Hwang, S. S.; Ober, C. K.; Perutz, S.; Iyengar, D.; Schneggenburger, L. A.; Kramer, E. J. *Polymer* **1995**, *36*, 1321. Iyengar, D. R.; Perutz, S. M.; Dai, C.-A.; Ober, C. K.; Kramer, E. J. *Macromolecules* **1996**, *29*, 1229.

(5) Cai, Y.; Gardner, D.; Caneba, G. T. *J. Adhes. Sci. Technol.* **1999**, *13*, 1017. Chen, X.; Gardella, J. A., Jr. *Macromolecules* **1994**, *27*, 3363.

(6) Schmidt, D. L.; DeKoven, B. M.; Coburn, C. E.; Potter, G. E.; Meyers, G. F.; Fischer, D. A. *Langmuir* **1996**, *12*, 518.

(7) Wang, J.; Mao, G.; Ober, C. K.; Kramer, E. J. *Macromolecules* **1997**, *30*, 1906.

(8) Genzer, J.; Sivaniah, E.; Kramer, E. J.; Wang, J.; Körner, H.; Xiang, M.; Yang, S.; Ober, C. K.; Char, K.; Chaudhury, M. K.; DeKoven, B. M.; Bubeck, R. A.; Fischer, D. A.; Sambasivan, S. In *Applications of Synchrotron Radiation Techniques to Materials Science IV*; Mini, S. M., Perry, D. L., Stock, S. R., Terminello, L. J., Eds.; Materials Research Society Symposium Proceedings, Vol. 524; Materials Research Society: Pittsburgh, PA 1998; p 365. Genzer, J.; Sivaniah, E.; Kramer, E. J.; Wang, J.; Körner, H.; Xiang, M.; Char, K.; Ober, C. K.; Chaudhury, M. K.; DeKoven, B. M.; Bubeck, R. A.; Sambasivan, S.; Fischer, D. A. *Macromolecules* **2000**, *33*, 1882.

(9) (a) Butoi, C. I.; Mackie, N. M.; Barnd, J. L.; Fisher, E. R.; Gamble, L. J.; Castner, D. G. *Chem. Mater.* **1999**, *11*, 862. (b) Castner, D, G.; Lewis, K. B., Jr.; Fischer, D. A.; Ratner, B. D.; Gland, J. L. *Langmuir* **1993**, *9*, 537.

(10) Xiang, M.; Li, X.; Ober, C. K.; Char, K.; Genzer, J.; Sivaniah, E.; Kramer, E. J., in press.

(11) ^1H NMR was used to determine the attachment ratio of the SF monodendrons in the SF-PI block. To enhance the solubility of such a polymer, a mixed solvent of deuterated chloroform and trifluorotrichloroethane (50/50 v/v) and elevated temperature of 40 °C were used. The relaxation time of 6 s was used for all polymer ^1H NMR characterization. The concentration of polymer for this study was kept at 5−10 mg/mL.

(12) Graupe, M.; Koini, T.; Wang, V. Y.; Nassif, G. M.; Colorado, R.; Villazana, R. J.; Dong, H.; Miura, Y. F.; Shmakova, O. E.; Lee, T. R. *J. Fluor. Chem.* **1999**, *93*, 107.

(13) Colorado, R., Jr.; Lee, T. R.; Genzer, J.; Sivaniah, E.; Kramer, E. J.; Char, K.; Ober, C. K.; Bubeck, R. A.; Fischer, D. A. Manuscript in preparation.

(14) Stöhr, J. *NEXAFS Spectroscopy*; Springer-Verlag: Berlin, 1992.

(15) Jäger, B.; Schürmann, H.; Müller, H. U.; Himmel, H.-J.; Neumann, M.; Grunze, M.; Wöll, C. *Z. Phys. Chem.* **1997**, *202*, 263. Wirde, M.; Gelius, U.; Dunbar, T.; Allara, D. L. *Nucl. Instr. Methods Phys. Res. B* **1997**, *131*, 245. Zharnikov, M.; Geyer, W.; Gölzhäuser, A.; Frey, S.; Grunze, M. *Phys. Chem. Chem. Phys.* **1999**, *1*, 3163.

(16) Certain commercial equipment is identified in this article in order to specify adequately the experimental procedure. In no case does such identification imply recommendation or endorsement by the National Institute of Standards and Technology, nor does it imply that the items identified are necessarily the best available for the purpose.

(17) Zisman, W. A. In *Contact angle, wettability, and adhesion*; American Chemical Society: Washington, DC, 1964.

(18) The following liquids (surface tensions in mJ/m^2) were used to measure θ for the Zisman plots: tetradecane (26.7), dodecane (25.4), decane (23.9), nonane (22.9), octane (21.8), heptane (20.3), silicone oil DMS-T01 (17.4), and silicone oil DMS-T00 (15.8).

(19) Outka, D.; Stöhr, J.; Rabe, J.; Swalen, J. D. *J. Chem. Phys.* **1988**, *88*, 4076.
(20) Genzer, J.; Sivaniah, E.; Kramer, E. J.; Wang, J.; Char, K.; Ober, C. K.; DeKoven, B. M.; Fischer, D. A. Manuscript in preparation.
(21) Matsen, M. W. *J. Chem. Phys.* **1997**, *106*, 7781 and references therein; *Curr. Opin. Colloid Interface Sci.* **1998**, *3*, 40 and references therein.
(22) Genzer, J.; Sivaniah, E.; Kramer, E. J.; Xiang, M.; Char, K.; Ober, C. K.; Wang, J.; Graupe, M.; Colorado, R., Jr.; Shmakova, O. E.; Lee, T. R.; Chaudhury, M. K.; M.; Bubeck, R. A.; Sambasivan, S.; Fischer, D. A. *Bull. Am. Phys. Soc.* **1999**, *44*, 1451.
(23) Lenk, T. J.; Hallmark, V. M.; Hoffmann, C. L.; Rabolt, J. F.; Castner, D. G.; Erdelen, C.; Ringsdorf, H. *Langmuir* **1994**, *10*, 4610.
(24) Tsao, M.-W.; Hoffmann, C. L.; Rabolt, J. F.; Johnson, H. E.; Castner, D. G.; Erdelen, C.; Ringsdorf, H. *Langmuir* **1997**, *13*, 4317.
(25) Grunze, M. *Phys. Scr.* **1993**, *T49*, 711.
(26) Nemetz, A.; Fischer, T.; Ulman, A.; Knoll, W. *J. Chem. Phys.* **1993**, *98*, 5912.
(27) Ulman, A. *Chem. Rev.* **1996**, *96*, 1533.

MA991710W